A Magnetic Field Detection and Localization Scheme for Internet of Underwater Things

Kwang-Yul Kim and Yoan Shin*
School of Electronic Engineering
Soongsil University, Seoul 06978, Korea
(*Corresponding author: yashin@ssu.ac.kr)

***Abstract*—The magnetic field whose intensity is changed by the magnetic permeability of the medium can be considered as a new underwater communication method. However, the magnetometer in the base station must compensate for the geomagnetic field to detect the underwater moving node for the communication and the localization. Therefore, this paper proposes a magnetic field detection and a localization scheme based on the exponential smoothing method. Simulation results show that the proposed scheme can extend the detection range and improve the localization accuracy by considering the trend of the geomagnetic field.**

***Index Terms*—internet of underwater things, magnetic field detection, localization, exponential smoothing, forecast**

I. Introduction

The sea is a large and deep unknown area. Although the seabed resources and biological resources are very abundant, the water pressure limits the underwater exploration by human. As a result, many countries are actively studying the internet of underwater things (IoUT) [1], which can link underwater infrastructures to obtain underwater information on the ground. However, in order to clearly observe the phenomenon occurring in the underwater, the underwater sensors should be able to approach into the close range, not to sense the situation from a long distance. Therefore, IoUT needs to be able to estimate the location of the underwater moving nodes (UMN).

Since the magnetic field can guarantee the same transmission performance on the ground, the magnetic induction communication applying to underwater has been studied [2]. However, since the magnetic field induction communication does not have propagation characteristics unlike underwater acoustic communication, the communication transmits the data only within a magnetic field range. Therefore, the UMNs must be located close to each other in order to guarantee the magnetic field induction communication. To this end, the magnetic field detection and the localization scheme are required. In this paper, we propose a magnetic field detection and localization scheme as a basic study of mobile underwater magnetic field induction communication for IoUT. Simulation results show that the proposed scheme can compensate for the geomagnetic field, extend the detection range, and improve the accuracy of localization by considering the trend of the geomagnetic field.

II. System Model

A. Magnetic Field Model

In this paper, we consider that an UMN is approaching to transmit the data to the underwater base station and three-axis magnetic vector sensors detect and estimate the location of the UMN. The magnetic field generated by the UMN can be modeled by the Biot-Savart's law as [3]

$$\begin{bmatrix} \widetilde{B_{x,\ell}} \\ \widetilde{B_{y,\ell}} \\ \widetilde{B_{z,\ell}} \end{bmatrix} = \frac{\mu_0}{4\pi d_\ell^5} \begin{bmatrix} 3x_\ell^2 - d_\ell^2 & 3x_\ell y_\ell & 3x_\ell z_\ell \\ 3x_\ell y_\ell & 3y_\ell^2 - d_\ell^2 & 3y_\ell z_\ell \\ 3x_\ell z_\ell & 3y_\ell z_\ell & 3z_\ell^2 - d_\ell^2 \end{bmatrix} \begin{bmatrix} M_x \\ M_y \\ M_z \end{bmatrix}, \tag{1}$$

where x_ℓ, y_ℓ, z_ℓ $(\ell = 1, \cdots, L)$ are the three-dimensional position in each sample of the UMN, L is the total number of samples, $\widetilde{B_{k,\ell}}$ [nT] is the k-axis magnetic field generated at the ℓ-th position, and M_k [Am^2] is the k-axis dipole moment of the UMN. $d_\ell = \sqrt{x_\ell^2 + y_\ell^2 + z_\ell^2}$ is the linear distance at the ℓ-th position between the magnetic vector sensor and the UMN, k_ℓ is the k-axis distance component between the ℓ-th position and sensor position, $\mu_0 = 4\pi \times 10^{-7}$ [H/m] is the permeability.

The magnetic field measured by the underwater sensor includes not only the magnetic field of the UMN but also the noise of the geomagnetic field and the thermal noise. Therefore, the measured magnetic field B_k can be finally expressed as

$$B_k = \widetilde{B_{k,\ell}} + G_k + N_k, \tag{2}$$

where G_k denotes the background geomagnetic noise, and N_k denotes the thermal noise of the magnetic vector sensor of the k-axis. Thus, it is necessary to compensate for the background geomagnetic field to improve the magnetic field detection performance and to detect only the magnetic field component of the UMN by minimizing the thermal noise.

B. Geomagnetic Compensation Method

In order to detect the UMN, the geomagnetic field must be compensated [3]. The representative method to compensate for the geomagnetic field is single exponential smoothing (SES). The SES can be expressed as [4]

$$\widehat{B_k^S}(t) = \gamma(t) \cdot B_k(t) + \{1 - \gamma(t)\} \cdot \widehat{B_k^S}(t-1), \tag{3}$$

where $\gamma(t)$ is the SES coefficient. If the difference between the measured magnetic fields is greater than the smoothing

threshold, the SES coefficient is adjusted as [4]

$$\gamma(t) = 0.1 \cdot [1/\{B_k(t) - B_k(t-1)\}] \cdot T_\gamma. \quad (4)$$

Hence, the magnitude of the magnetic field with the geomagnetic field compensated by SES is expressed as [4]

$$S(t) = \sqrt{\widehat{S_x}(t)^2 + \widehat{S_y}(t)^2 + \widehat{S_z}(t)^2}, \quad (5)$$

where $\widehat{S_k}(t) = B_k(t) - \widehat{B_k^S}(t)$. In order to detect the UMN, the detection threshold T_h^S is set by calculating the false alarm rate during the absence of the UMN, then the magnetic field is detected according to the threshold.

III. Proposed Scheme

The proposed scheme consists of the two steps: detecting the magnetic field and estimating the location of UMN.

A. Phase 1: Magnetic Field Detection

The geomagnetic field is mostly generated by the flow of electric current inside the Earth. The geomagnetic field is changed in real-time by the electronic equipment generated around the magnetic sensor including the solar wind. On the other hand, there is no way to accurately model the geomagnetic field in real-time. However, experimental studies have been carried out in consideration of the trend of the geomagnetic field when modeling the magnetic field [5]. Therefore, this paper assumes that there is a trend in the geomagnetic field and chooses the double exponential smoothing (DES) method which can consider the trend among the time series analysis method [6]. The DES can be expressed as [6]

$$\widehat{B_k^D}(t) = \alpha \cdot B_k(t) + (1-\alpha) \cdot \left\{ \widehat{B_k^D}(t-1) + T_k(t-1) \right\}, \quad (6)$$

$$T_k(t) = \beta \cdot \left\{ \widehat{B_k^D}(t) - \widehat{B_k^D}(t-1) \right\} + (1-\beta) \cdot T_k(t-1), \quad (7)$$

where $\widehat{B_k^D}(t)$ is the smoothed k-axis magnetic field, $T_k(t)$ is the k-axis trend value, α $(0 < \alpha < 1)$ is the DES coefficient, and β $(0 < \beta < 1)$ is the trend coefficient. In order to compensate and detect in real-time, we constructed the window filter $\mathbf{W}_k(t)$ as

$$\mathbf{W}_k(t) = \left[\widehat{B_k^D}(t-M+1), \cdots, \widehat{B_k^D}(t-M+N), \cdots, \widehat{B_k^D}(t) \right], \quad (8)$$

where M is the total filter length, N is the number of smoothed magnetic field used to forecast. If there is a magnetic field from the UMN, a large difference occurs because both the smoothed magnetic field and the predicted magnetic field show increasing or decreasing straight lines. On the other hand, if there is only the geomagnetic field, the predicted magnetic field crosses or approaches the smoothed magnetic field. Thus, the magnetic field can be detected by comparing the difference between the smoothed magnetic field and the predicted magnetic field. Thus, the detection filter $\mathbf{D}_k(t)$ can be expressed as

$$\mathbf{D}_k(t) = \begin{bmatrix} \widehat{\mathbf{B}_k^D}(t) \\ \mathbf{F}_k(t) \end{bmatrix} = \begin{bmatrix} \widehat{B_k^D}(t+1-m), \cdots, \widehat{B_k^D}(t) \\ F_k(t+1-m), \cdots, F_k(t) \end{bmatrix}. \quad (9)$$

where $F_k(t+1-m) = \widetilde{B_k^D}(t+1-m) + mT_k(t+1-m)$ is the predicted magnetic field and m is the number of the predicted magnetic field. Thus, the magnetic field of the proposed scheme to detect the UMN can be expressed as

$$F(q) = \min_{q \in \{t+1-m, \cdots, 1\}} \sqrt{\widehat{F_x}(q)^2 + \widehat{F_y}(q)^2 + \widehat{F_z}(q)^2}, \quad (10)$$

Here, $\widehat{F_k}(q) = F_k(q) - \widehat{B_k^D}(q)$. In order to measure the presence of the UMN, the detection threshold T_h^D is set by calculating the false alarm rate during the absence of the UMN, and the magnetic field is detected according to the threshold.

B. Phase 2: Magnetic Field Localization

Since the magnetic field does not have the characteristic of propagating far away, the time-of-arrival (ToA) method can not be used. Moreover, if the location of the sensor that detects the magnetic field is directly estimated as the location of the UMN, a large localization error may occur since the magnetic field has the exponential characteristic according the the distance. Hence, it is necessary to judge whether the UMN is entering the sensor network. Determination of whether or not the UMN enters the sensor network can be expressed as

$$P = \begin{cases} 1 & \text{if } \frac{1}{J} \sum_{j=1}^{J} Y_j(t) \geqslant T_h^P \\ 0 & \text{if } \frac{1}{J} \sum_{j=1}^{J} Y_j(t) < T_h^P \end{cases}, \quad (11)$$

where J is the number of deployed anchor nodes (ANs), $Y_j(t)$ is the smoothed magnitude of the magnetic field of the j-th AN, T_h^P is the threshold for determining the entrance, and P is the entrance result. In this case, T_h^P can be adjusted by considering the maximum value of the magnitude of the magnetic field that varies with the dipole moment. Then, the location estimation according to entrance result P can be expressed as

$$\mathbf{XY}(t) = \begin{cases} \text{find}(Y_j(t) \geqslant T_h^P) & \text{if } P=0 \\ \text{find}(Y_j(t) \geqslant \frac{1}{J} \sum_{j=1}^{J} Y_j(t) T_h^P) & \text{if } P=1 \end{cases}, \quad (12)$$

where find$(\cdot)$ is a function to find the AN position, and $\mathbf{XY}(t)$ denotes the 2-dimensional positions of the ANs at t [sec]. Finally, the estimated location $\widehat{XY}(t) = E[\mathbf{XY}(t)]$.

IV. Simulation Results

Since there is a physical limitation to evaluate the detection and localization perform in real underwater environments, we measured the geomagnetic field on the ground. In order to evaluate the detection performance, the magnetic field was generated by superimposing the modeled magnetic field using (1) on the geomagnetic field measured at dawn. The three-axis dipole moment of the UMN is $\{54, 28.3, 88.6\}$, the movement velocity is 1 [m/sec], and movement depth is 0 [m]. The UMN moves on-top of a sensor in the sensor network line. The sensor deployment distance is 10 [m], and the deployed depth is 20 [m]. We assume that the three-axis of all sensors are aligned. We considered the SES coefficient $\gamma = 0.1$, the DES coefficient $\alpha = 0.1$, the trend coefficient $\beta = 0.94$, the filter length $M = 52$ [sec], and the forecasting number $m = 7$ [sec].

Figure 1 shows the initial and total detection distances according to the detection threshold in an ideal environment. The figure shows that the DES scheme can extend the detection range of the SES scheme.

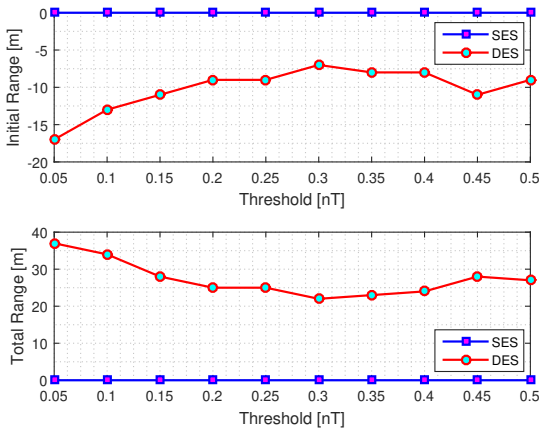

Fig. 1. Ideal detection range according to the detection threshold

A. Detection Performance

In order to evaluate the performance, we calculate the false alarm rate P_{fa} and simulate 1,000 times using different section of the measured geomagnetic field with T_h^D when P_{fa}=10^{-2}. Figure 2 shows the false alarm rate according to the threshold and detection probability according to time. From the detection probability result, we can observe that the proposed scheme is sensitive to the geomagnetic field trend, which can shorten the initial detection time and extend the total detection time. Through the simulation results, we observe the proposed scheme can improve the detection range by considering the trend of the geomagnetic field.

B. Localization Performance

In order to evaluate the localization accuracy, we consider the deployment distance between each AN is 2∼10 [m] and

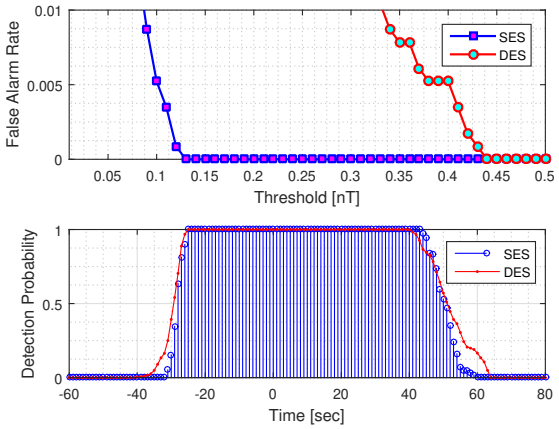

Fig. 2. False alarm rate (top) and detection probability (bottom)

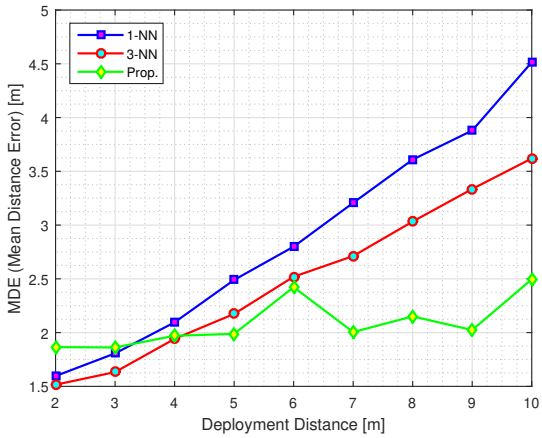

Fig. 3. MDE performance

CPA (Closest Proximity Approach) is 10 [m]. Figure 3 shows the mean distance error (MDE) according to the deployment distance. We consider the k-NN (Nearest Neighbor) [7] to compare the performance. From the simulation results, it is expected that the proposed scheme can design the cost-effective localization system than the 1-NN and 3-NN schemes by considering the characteristics of the magnetic field.

V. Conclusions

In this paper, we proposed the magnetic field detection scheme and the localization scheme for the mobile underwater magnetic field induction communication which can be considered in IoUT. The proposed scheme improves the detection range by considering the trend of the geomagnetic field and can improve the localization accuracy. In the further work, we will study the method of estimating the location of multiple UMNs using the clustering method.

Acknowledgment

This work was supported by the NRF grant funded by the Korea government (MSIT) (2016R1A2B2014497).

References

[1] M. C. Domingo, "An overview of the internet of underwater things," *Jour. Network Comput. Appl.*, vol. 35, no. 6, pp. 1879-1890, Nov. 2012.

[2] I. F. Akyildiz, P. Wang, and Z. Sun, "Realizing underwater communication through magnetic induction," *IEEE Commun. Mag.*, vol. 53, no. 11, pp. 42-48, Nov. 2015.

[3] A. Sheinker, L. Frumkis, B. Ginzburg, N. Salomonski, and B.-Z.Kaplan, "Magnetic anomaly detection using a three-axis magnetometer," *IEEE Trans. Magn.*, vol. 45, no. 1, pp. 160-167, Jan. 2009.

[4] M. Kim, U. Joo, C. Lim, S. Yoon, and S. Moon, "A study on detection of underwater ferromagnetic target for harbor surveillance," *Jour. KIMST*, vol. 18, no. 4. pp. 350-357, Aug. 2015.

[5] J. B. Nelson and T. C. Richards, *Magnetic Source Parameters of MR OFFSHORE Measured during Trial MONGOOSE 07*, Defense R&D Canada-Atlantic, DRDC Atlantic TM 2007-223, Sept. 2007.

[6] E. S. Gardner Jr. "Exponential smoothing: The state of the art - Part II," *Int. Jour. Forecast*, vol. 22, no. 4, pp. 637-666, Oct. 2006.

[7] A. Kushki, K. N. Plataniotis, and A. N. Venetsanopoulos, *WLAN Positioning System: Principles and Applications in Location-Based Services*, Cambridge University Press, 2012.